

Published in final edited form as:

Heart Rhythm. 2012 October ; 9(10): 1698–1705. doi:10.1016/j.hrthm.2012.06.031.

New experimental evidence for mechanism of arrhythmogenic membrane potential alternans based on balance of electrogenic I_{NCX} / I_{Ca} currents

Xiaoping Wan, MD, PhD¹, Michael Cutler, DO, PhD¹, Zhen Song, BS², Alain Karma, PhD², Toshio Matsuda, PhD³, Akemichi Baba, PhD³, and David S. Rosenbaum, MD, FHRS^{1,*}

¹The Heart and Vascular Research Center, MetroHealth Campus, Case Western Reserve University, Cleveland, Ohio

²Physics Department and Center for Interdisciplinary Research on Complex Systems, Northeastern University, Boston, Massachusetts

³Graduate School of Pharmaceutical Sciences, Osaka University, Japan

Abstract

Background—Computer simulations have predicted that the balance of various electrogenic sarcolemmal ion currents may control the amplitude and phase of beat-to-beat alternans of membrane potential (V_m). However, experimental evidence for the mechanism by which alternans of calcium transients produces alternation of V_m (V_m -ALT) is lacking.

Objective—We sought to provide experimental evidence that Ca-to- V_m coupling during alternans is determined by the balanced influence of two Ca-sensitive electrogenic sarcolemmal ionic currents, I_{NCX} and I_{Ca} .

Methods and Results— V_m -ALT and Ca-ALT were measured simultaneously from isolated guinea pig myocytes ($n=41$) using perforated patch and Indo-1_{AM} fluorescence, respectively. There were three study groups: 1) Control, 2) I_{NCX} predominance created by adenoviral-induced NCX overexpression, and 3) I_{Ca} predominance created by I_{NCX} inhibition (SEA-0400) or enhanced I_{Ca} (As_2O_3). During alternans, 14 of 14 control myocytes demonstrated positive Ca-to- V_m coupling, consistent with I_{NCX} , but not I_{Ca} as the major electrogenic current in modulating action potential duration. Positive Ca-to- V_m coupling was maintained during I_{NCX} predominance in 8 of 8 experiments with concurrent increase in Ca-to- V_m gain ($p<0.05$), reaffirming the role of increased forward mode electrogenic I_{NCX} . Conversely, I_{Ca} predominance produced negative Ca-to- V_m coupling in 14 of 19 myocytes ($p<0.05$) and decreased Ca-to- V_m gain compared to control ($p<0.05$). Furthermore, computer simulation demonstrated that Ca-to- V_m coupling changes from negative to positive was due to a shift from I_{Ca} to I_{NCX} predominance with increasing pacing rate.

© 2012 The Heart Rhythm Society. Published by Elsevier Inc. All rights reserved.

Address correspondence to: Xiaoping Wan, PhD, MD, Heart and Vascular Research Center, MetroHealth Campus, Case Western Reserve University, Rammelkamp, 6th Floor, #643, 2500 MetroHealth Drive, Cleveland, Ohio 44109-1998, Tel: (216) 778-7496, Fax: (216) 778-1261, xwan@metrohealth.org.

*Deceased

Publisher's Disclaimer: This is a PDF file of an unedited manuscript that has been accepted for publication. As a service to our customers we are providing this early version of the manuscript. The manuscript will undergo copyediting, typesetting, and review of the resulting proof before it is published in its final citable form. Please note that during the production process errors may be discovered which could affect the content, and all legal disclaimers that apply to the journal pertain.

Disclosures: None

Conclusion—These data provide the first direct experimental evidence that coupling in phase and magnitude of Ca-ALT to Vm-ALT is strongly determined by relative balance of prominence of I_{NCX} versus I_{Ca} currents.

Keywords

alternans; repolarization; action potentials; intracellular calcium

INTRODUCTION

Microvolt-level T wave alternans is a sensitive marker of vulnerability to ventricular arrhythmias in patients^{1, 2}. T-wave alternans of the surface ECG arises from beat to beat alternation of action potential duration (Vm-ALT) at the single cell level. Under this paradigm beat-to-beat alternation of the calcium transient (Ca-ALT) causes beat-to-beat alternans in action potential shape and duration (Vm-ALT)³⁻⁵. This concept was supported by our previous findings showing close correspondence between myocytes exhibiting depressed expression or function of calcium cycling proteins and their susceptibility to Vm-ALT³. Therefore determining the mechanism by which electrogenic ionic currents transform Ca-ALT to Vm-ALT is critical to understanding how cardiac alternans promotes electrophysiological heterogeneities and cardiac arrhythmias. Previously computer simulations have predicted that the balance of various electrogenic sarcolemmal ion currents may control the amplitude and phase of beat-to-beat alternans of membrane potential⁵⁻⁸. However, to our knowledge these theoretical predictions have not been tested experimentally. We hypothesized that Ca-to-Vm coupling during alternans (i.e., the relationship between alternating calcium transients and the corresponding phase and amplitude of action potential alternans) is determined by the balanced influence of two Ca-sensitive electrogenic sarcolemmal ionic currents, I_{NCX} and I_{Ca} . This hypothesis is based on established sensitivity of these currents to cytoplasmic calcium concentration. During Ca-ALT, a large calcium release is expected to promote forward mode I_{NCX} , hence prolonging APD, whereas this will be opposed by calcium induced inactivation of I_{Ca} , which shortens APD. Therefore, the relative predominance of each current would determine how Ca-ALT is coupled with respect to gain and phase to Vm-ALT. We used complementary and selective approaches to modify I_{NCX} or I_{Ca} function and hence to examine Ca-to-Vm coupling sign and Ca-to-Vm gain under conditions of I_{NCX} vs. I_{Ca} predominance. Our data supported the hypothesis that Ca-to-Vm coupling is determined by a competing balance of I_{NCX} (positive Ca-to-Vm coupling) and I_{Ca} (negative Ca-to-Vm coupling), and demonstrated that I_{NCX} is the major electrogenic mechanisms of Vm-ALT. These findings also have implications for disease states where the balance of ion channel expression is altered.

METHODS

Study Design

Myocytes were divided into three groups to investigate the competing balanced influence of two Ca-sensitive electrogenic sarcolemmal ionic currents, I_{NCX} and I_{Ca} on Ca-to-Vm coupling during alternans: 1) Control, 2) I_{NCX} predominance, and 3) I_{Ca} predominance. I_{NCX} predominance was achieved by In-vivo NCX gene transfer using a modified cross-clamping method⁹. Western blot from in vitro NCX overexpression showed that NCX protein expression was indeed increased by 3.8 ± 2.9 folds compared to control (n=3) and previously Ranu et al demonstrated that overexpression of NCX increases I_{NCX} , with no change in I_{Ca} .¹⁰ I_{Ca} predominance was achieved by I_{NCX} inhibition or I_{Ca} enhancement. One μ M of the selective I_{NCX} inhibitor SEA0400 (Taisho Pharmaceutical Co, Ltd, Saitama, Japan) was used to achieve 80% I_{NCX} inhibition with no change in I_{Ca} ^{11, 12}. I_{Ca} was

increased with As_2O_3 ¹³. Myocytes were studied after 4 hours incubation with 3 μM of As_2O_3 . The procedure increased I_{Ca} density by about 100% with no significant effect on I_{NCX} under our experimental condition (see supplemental data).

Vm-ALT and Ca-ALT recordings

As described in supplementary material, Vm-ALT and Ca-ALT were measured simultaneously from isolated guinea pig myocytes ($n=41$) using perforated patch and Indo-1_{AM} fluorescence, respectively. All experiments were performed at 32°C. Vm-ALT amplitude was measured by calculating the ratio of the difference in action potential duration (APD₉₀) to the average APD₉₀ for two consecutive beats. Ca-ALT amplitude was measured by calculating the ratio of the difference in Ca transient amplitude to the average Ca transient amplitude for two consecutive beats. Ca-to-Vm coupling was determined from the coincident phase of Vm-ALT to Ca-ALT (i.e. positive vs. negative Ca-to-Vm coupling) and Ca-to-Vm gain was calculated as the ratio of Vm-ALT to Ca-ALT.

I_{Ca} recordings

I_{Ca} were elicited from a holding potential of -40 mV with depolarizing voltage pulses to 0 mV for 140 ms. Stimulation protocol, solutions, and temperature were the same as for V-ALT recordings.

Computer simulations

Computer simulations were performed using a guinea pig ventricular myocyte model that was constructed by combining mathematical formulations of selected sarcolemmal currents from¹⁴ together with a mathematical model of Ca handling from¹⁵ (see supplementary material for the detail) that produces CaT alternans. To study how the pacing rate and the balance of I_{NCX} and I_{Ca} influence Ca-to-Vm gain, we performed simulations for the control case and I_{Ca} predominance. The latter case was simulated by decreasing the maximum strength of I_{NCX} by 80%. Simulations were also carried out using the rabbit ventricular myocyte model of Mahajan et al¹⁵ in order to demonstrate the robustness of electrogenic mechanisms underlying Ca-to-Vm coupling in different mammalian species (shown in the supplemental material).

Statistical analysis

Statistical analysis of data was performed using Sigastat (SPSS Inc., Chicago, Illinois, USA). Statistical differences were assessed with One way ANOVA. A $p<0.05$ was considered statistically significant. Results were expressed as mean \pm standard error of the mean (SEM).

RESULTS

Effect of I_{NCX} versus I_{Ca} predominance on calcium to voltage coupling during alternans

To examine the influence of I_{NCX} and I_{Ca} on Ca-to-Vm coupling during alternans, action potentials (V) and calcium transients (Ca) alternans were simultaneously recorded as shown in Figure 1. In the control myocyte (top left) Ca-to-Vm coupling was positive; i.e., large Ca transient amplitude was coupled with long APD whereas small Ca transient amplitude was coupled with short APD on subsequent beat, consistent with I_{NCX} , but not I_{Ca} as the major electrogenic current. Consistent with this observation, with NCX overexpression (top right) positive Ca-to-Vm coupling was maintained with a concurrent increase in Ca-to-Vm gain, i.e. the ratio of Vm-ALT to Ca-ALT was larger than in control myocyte (0.62 vs 0.2 in these examples), confirming increased forward mode electrogenic I_{NCX} . In contrast, I_{Ca} predominance induced by inhibiting I_{NCX} with SEA0400 (1 μM) (bottom left) or increasing

I_{Ca} with As_2O_3 (bottom right) produced negative Ca-to-Vm coupling at 240 bpm, i.e. small Ca transient amplitude was coupled with long APD whereas large Ca transient amplitude was coupled with short APD on subsequent beat. The gain is small and negative (-0.13 and -0.09 respectively in these examples). These results are summarized in the Table. All control myocytes (14 of 14) demonstrated positive Ca-to-Vm coupling, consistent with I_{NCX} , but not I_{Ca} as the major electrogenic current. Positive Ca-to-Vm coupling was maintained with NCX overexpression in 8 of 8 myocytes with concurrent increase in Ca-to-Vm gain, confirming increased electrogenic I_{NCX} . Conversely, I_{Ca} predominance produced negative Ca-to-Vm coupling in 10 of 11 myocytes with inhibited NCX and 4 of 8 myocytes with increased I_{Ca} . The bottom panel in Figure 1 shows the negative Ca-to-Vm coupling examples. These data provide direct experimental support to our hypothesis that coupling in phase and magnitude of Ca-ALT to Vm-ALT is strongly determined by relative balance of prominence of I_{NCX} versus I_{Ca} currents.

Effect of I_{NCX} versus I_{Ca} predominance on Ca-to-Vm gain during alternans

To specifically examine the balanced influence of I_{NCX} and I_{Ca} on Ca-to-Vm gain during alternans, the ratio of Vm-ALT to Ca-ALT was calculated and plotted in Figure 2. The figure showed that increased I_{NCX} predominance by overexpressing NCX increased Ca-to-Vm gain ($n=8$, $p < 0.05$ compared to control $n=14$) indicating that relative availability of forward mode I_{NCX} is an important driving force for Vm-ALT. Conversely, at pacing rate of 240 bpm, enhancing I_{Ca} predominance by inhibiting I_{NCX} with SEA0400 decreased Ca-to-Vm gain significantly ($n=11$, $p < 0.05$ compared to control $n=14$). There was a trend towards increasing I_{Ca} with As_2O_3 also decreased Ca-to-Vm gain, but not significantly ($n=8$, $p=0.09$ compared to control $n=14$). Therefore, Ca-to-Vm gain is strongly influenced by the balance of electrogenic I_{NCX} / I_{Ca} currents. However, at faster pacing rate (333 bpm) there was no difference in Ca-to-Vm gain between control and enhancing I_{Ca} predominance groups.

Effect of pacing rate on Ca-to-Vm coupling during alternans

Since current density of I_{Ca} but not I_{NCX} is influenced by recovery from time-dependent inactivation, increasing pacing rate is expected to reduce I_{Ca} current relative to I_{NCX} . Hence, we varied pacing rate to shift the relative contribution of I_{Ca} versus I_{NCX} as a means of further testing how the balance of these currents influences the transduction of Ca-ALT to Vm-ALT. Unlike control conditions, only under conditions of I_{Ca} preponderance (Figure 3, left panels) we observed negative Ca-to-Vm coupling. However, at faster pacing rates (Figure 3, right panels) Ca-to-Vm coupling became positive suggesting that the balance of I_{NCX} and I_{Ca} was shifted in such a way that I_{Ca} may no longer be the predominant electrogenic current in modulating action potential duration. This was further explored in the computer simulation shown in figure 4 where rate-dependence of Ca-to-Vm gain is plotted under control versus conditions of I_{Ca} preponderance (decreased I_{NCX}). Consistent with our experimental results, Ca-to-Vm coupling was always positive in controls (Figure 4 filled rectangles), and Ca-to-Vm coupling increased as heart rate increased, consistent with rate-dependent inactivation of I_{Ca} but not I_{NCX} (i.e. further enhancing I_{NCX} preponderance). Correspondingly, negative Ca-to-Vm coupling was observed only after shifting to conditions of I_{Ca} preponderance (Figure 4 open rectangles). However, as heart rate increased there was a reversion to positive Vm-to-Ca coupling, completely mirroring our experimental results (Figure 3).

To further explore the mechanism for dynamic shifts from negative to positive Vm-to-Ca coupling, we examined the traces of action potential, Ca transient, I_{Ca} and I_{NCX} at pacing rate of 240 bpm (left), 300 bpm (middle), and 333 bpm (right) in a condition where I_{NCX} is inhibited by 80%. The results of those computer simulations are shown in Figure 5 (a, b, c). Since action potential duration is influenced by the total amount of Ca influx through I_{Ca}

and the peak I_{NCX} current density, we report for each current time trace numerical values for the time integrated value of I_{Ca} during the action potential (in $(pA/pF)*ms$), and the peak I_{NCX} value. Ca-to-Vm coupling was negative with inhibited I_{NCX} at a pacing rate of 240 bpm (left). As pacing rate increased to 333 bpm, Ca-to-Vm coupling became positive (right). However, at pacing rate of 300 bpm, there was large Ca-ALT but virtually no Vm-ALT. At a pacing rate of 240 bpm, I_{Ca} amplitude was large because of reduced Ca-dependent inactivation of this current when the Ca T amplitude is small, consistent with I_{Ca} predominance producing negative Ca-to-Vm coupling. As pacing rate increased to 333 bpm, I_{Ca} predominance was reduced due to shortening of APD but peak I_{NCX} magnitude increased due to increase Ca loading. Interestingly, at a pacing rate of 300 bpm, a smaller Ca T still corresponded to a larger I_{Ca} . However the difference of time-averaged I_{Ca} values between two beats were smaller than those at 240 bpm, thereby decreasing the contribution of I_{Ca} to Vm-ALT. In addition, average I_{NCX} was increased at 300 bpm compared to 240 bpm, thereby increasing the contribution of I_{NCX} to Vm-ALT. At 300 bpm, the effect of Ca-ALT on I_{NCX} and I_{Ca} was almost completely balanced so that Vm-ALT were absent despite the presence of Ca-ALT. In this situation, CaT-ALT are “hidden” insofar that their existence could not be inferred from electrical measurement alone. For pacing rate smaller (larger) than 300 bpm, Ca-to-Vm coupling was negative (positive). Therefore as pacing rate increased, the change of Ca-to-Vm coupling from negative to positive was due to a shift from I_{Ca} to I_{NCX} predominance. However, for control experiments shown in Figure 6, a small Ca T induced a small peak I_{NCX} . Thus APD shortened although I_{Ca} increased due to reduced Ca induced I_{Ca} inactivation at 240 bpm. As pacing rate increased to 444 bpm, I_{NCX} magnitude further increased due to its Ca dependence but APD was too short for I_{Ca} to dominate. Ca-to-Vm coupling was positive at all pacing rates, consistent with I_{NCX} , but not I_{Ca} , being the major electrogenic current producing Vm-ALT from Ca-ALT.

Checking the relationship between I_{Ca} and CaT for both control and during I_{NCX} inhibition we found that small CaT were associated with large I_{Ca} at slower pacing rates while at faster pacing rates, small CaT were associated with small I_{Ca} . However, Ca-to-Vm coupling changes from negative to positive as pacing rate increased occurred only with I_{NCX} inhibition.

These two figures also demonstrated the rate dependence of I_{Ca} and I_{NCX} . At control condition, average I_{Ca} between two consecutive beats decreased as pacing rate increased ($417(pA/pF)*ms$, $341(pA/pF)*ms$, and $322(pA/pF)*ms$ at 240bpm, 333bpm, and 444bpm respectively) whereas average I_{NCX} between two consecutive beats increased as pacing rate increased ($-1.685pA/pF$, $-1.86pA/pF$, and $-2.115pA/pF$ at 240bpm, 333bpm, and 444bpm respectively). At inhibiting I_{NCX} (by 80%) condition, average I_{Ca} between two consecutive beats decreased as pacing rate increased ($256(pA/pF)*ms$, $237(pA/pF)*ms$, and $173(pA/pF)*ms$ at 240bpm, 300bpm, and 330bpm respectively) whereas average I_{NCX} between two consecutive beats increased as pacing rate increased ($-1.045pA/pF$, $-1.14pA/pF$, and $-1.245pA/pF$ at 240bpm, 300bpm, and 330bpm respectively). Figure 7 (top panel) shows representative traces of I_{Ca} at different pacing rate at patch-clamp experiments in real myocytes. As pacing rate increased I_{Ca} density decreased, confirming the results of computer simulations.

These data further support that as pacing rate increased the balance of I_{Ca} to I_{NCX} shift towards I_{NCX} predominance even under inhibiting I_{NCX} condition. Taken together, these finding reaffirmed that small shifts in the balance of I_{Ca} and I_{NCX} can influence Ca-to-Vm coupling during cardiac alternans.

DISCUSSION

In the present report, we provide new experimental evidence supporting an important role for a fine balance between electrogenic I_{NCX}/I_{Ca} currents in cardiac alternans. In particular, we find that I_{NCX} predominance produces positive Ca-to- V_m coupling whereas I_{Ca} predominance produces negative Ca-to- V_m coupling. When the effect of CaT-ALT on these two currents is perfectly balanced, CaT-ALT does not produce V_m -ALT (zero gain). In addition, the sign of Ca-to- V_m coupling can change with pacing rate due to the fact that I_{Ca} and I_{NCX} have different dependences. Combined with the theoretical framework provided by the computer simulations, our findings help to shed light on complex mechanisms controlling the relationship between cytosolic calcium and membrane voltage under highly dynamic conditions such as alternans which ultimately influence the spatial organization of repolarization in the heart.

Electrogenic mechanisms for transducing Ca-ALT to V_m -ALT

The central aim of this work was to establish experimental evidence for the mechanism by which the myocyte generates V_m -ALT from Ca-ALT. Elucidating this relationship is critical to understanding how arrhythmogenic V_m -ALT arises under normal and pathological conditions. There are several important electrogenic feedback mechanisms by which Ca-ALT can be transduced to V_m -ALT including; 1. SR calcium release enhances inactivation of sarcolemmal I_{Ca} , shown as negative feedback because it results in lowering membrane voltage (shortening APD), and 2. SR calcium release enhances calcium extrusion by I_{NCX} , shown as positive feedback because it increases membrane voltage (lengthens APD because electrogenic I_{NCX} drives 3 sodium into the cell for every one calcium extruded). It has been observed that the large Ca transient during beat-to-beat (large-small) Ca-ALT is accompanied by a short APD in some species (or certain experimental conditions)^{16, 17}, while in other species by a prolonged APD^{18, 19}. It was suggested that the I_{NCX} is responsible for prolongation of APD during large Ca transient, while Ca-dependent inactivation of I_{Ca} is the mechanism of APD shortening^{7, 18}.

Our data suggest that I_{NCX} is the most preponderant electrogenic mechanism for V_m -ALT, based on the fact that we consistently observed positive Ca-to- V_m coupling in normal myocytes in this (Figure 1) and prior studies.^{4, 20} In other words, under normal conditions, Ca-ALT and V_m -ALT are in phase. The opposite would be expected if I_{Ca} was the electrogenic mechanism. However, we also hypothesize that any condition (drugs, disease, heart rate, etc), which shifts the balance of sarcolemmal currents away from I_{NCX} preponderance, will also change the electrogenic currents that govern alternans, and hence the magnitude and phase of cellular alternans.

The balance of I_{NCX} and I_{Ca} determines the phase and gain of Ca-to- V_m coupling

The advantage of manipulating I_{NCX} and I_{Ca} predominances in the present study stems from the ability to demonstrate a causal relationship between a single current and the development of cellular alternans and Ca-to- V_m coupling. As shown in figure 1, I_{NCX} predominance produces positive Ca-to- V_m coupling whereas I_{Ca} predominance produces negative Ca-to- V_m coupling. Selective enhancement or reduction of I_{NCX} increased or decreased Ca-to- V_m gain, respectively as demonstrated in Figure 2. This finding supports the hypothesis that I_{NCX} is the principle electrogenic current for V_m -ALT. Conversely, when I_{NCX} was inhibited, I_{Ca} becomes the predominant electrogenic carrier transducing Ca-ALT to V_m -ALT. In this case, negative Ca-to- V_m coupling is observed to produce electromechanical discordance, where Ca transient and APD alternate in opposite phase (figure 1).

To check the importance of Ca-dependence of I_{Ks} , we repeated the simulations of Figure 4 after removing the Ca-dependence of I_{Ks} by replacing Ca_i by a constant value of 0.1 μM in the formula for g_{Ks} given in the supplementary material. The results were unchanged, showing that the Ca-dependence of I_{Ks} has a negligible role in determining the sign of Ca-to- V_m coupling.

The balance of I_{NCX} and I_{Ca} determining the gain of Ca-to- V_m coupling may also explain the differences of Ca-to- V_m gain between canine and guinea pig. It has been reported that the larger Ca-to- V_m gain in the canine compared with guinea pig is due to differences in ion channel expression levels and kinetic properties²¹. On the background of smaller I_{Kr} and I_{Ks} in the canine²², in conjunction with a much smaller I_{Ca} during the late AP plateau²³, Ca transient-induced changes in I_{NCX} have a much greater modulatory effect on AP repolarization, identifying I_{NCX} as the predominant Ca-to- V_m coupler during alternans. The other Ca-dependent currents, I_{Ca} and I_{to} , play a role in shaping the AP during its initial plateau phase, causing crossover between consecutive APs during alternans, but have a minimal effect on APD. The situation can be different, with I_{Ca} playing a role in V_m -ALT, in species, where I_{Ca} persists into the late phase of the AP (e.g., guinea pig) and the Ca-dependent I_{Ks} repolarizing current has a large conductance^{24, 25}. Under such conditions, a large Ca transient can lead to APD shortening during alternans, due to increased Ca-dependent inactivation of I_{Ca} . Therefore, the Ca-to- V_m coupling gain in the guinea pig is smaller compared with canine²¹ and the balance of I_{NCX} and I_{Ca} determines the gain of Ca-to- V_m coupling.

Our data also suggest that small shifts in the balance of activity between I_{NCX} and I_{Ca} can dynamically influence Ca-to- V_m coupling. Under conditions of I_{Ca} preponderance, negative coupling between Ca-ALT and V_m -ALT was transformed to positive coupling at increased heart rates (Figure 4). To explain the rate dependent shift we determined the rate dependence of I_{Ca} and I_{NCX} . I_{Ca} at different pacing rate were measured and shown in Figure 7. As pacing rate increased I_{Ca} density decreased. Since we used same square waveform to initiate I_{Ca} faster pacing rate means shorter diastolic interval for I_{Ca} to recover from inactivation and less channel available for the activation. Faster pacing also increases diastolic calcium. The rise in calcium at high rates depends primarily on the corresponding accumulation of sodium, due to the activity of I_{NCX} ²⁶. Another mechanism that promotes calcium loading at high rates is that the action potential waveform spends more time per period at plateau potentials, and so the time spent in the calcium efflux mode is reduced. Therefore, with increasing pacing rate, I_{NCX} increases and I_{Ca} decreases in normal myocytes. Pharmacological inhibition of I_{NCX} affects the rate dependences of both I_{Ca} decrease and I_{NCX} increase as shown in Figure 5&6, thereby shifting the balance of I_{NCX} and I_{Ca} in a rate-dependent fashion. For intermediate pacing rate (240 bpm), I_{Ca} dominates due to I_{NCX} inhibition, thereby giving rise to negative coupling. In contrast, for even faster pacing rate (333 bpm), the I_{Ca} decrease and I_{NCX} increase are sufficient to produce a positive coupling despite pharmacological I_{NCX} inhibition.

Supplementary Material

Refer to Web version on PubMed Central for supplementary material.

Acknowledgments

The virus (Ad.NCX) was the gift from Dr Hajjar's lab in Mount Sinai School of Medicine, USA.

Sources of Funding

This study was supported by a grant from the NIH (#RO1-HL54807, DSR). Zhen Song also acknowledges support of an AHA predoctoral fellowship.

Reference List

1. Ikeda T, Saito H, Tanno K, et al. T-wave alternans as a predictor for sudden cardiac death after myocardial infarction. *Am J Cardiol.* 2002; 89:79–82. [PubMed: 11779531]
2. Rosenbaum DS, Jackson LE, Smith JM, Garan H, Ruskin JN, Cohen RJ. Electrical alternans and vulnerability to ventricular arrhythmias. *N Engl J Med.* 1994; 330:235–241. [PubMed: 8272084]
3. Pruvot EJ, Katta RP, Rosenbaum DS, Laurita KR. Role of calcium cycling versus restitution in the mechanism of repolarization alternans. *Circ Res.* 2004; 94:1083–1090. [PubMed: 15016735]
4. Wan X, Laurita KR, Pruvot EJ, Rosenbaum DS. Molecular correlates of repolarization alternans in cardiac myocytes. *J Mol Cell Cardiol.* 2005; 39:419–428. [PubMed: 16026799]
5. Weiss JN, Karma A, Shiferaw Y, Chen PS, Garfinkel A, Qu Z. From pulsus to pulseless: The saga of cardiac alternans. *Circ Res.* 2006; 98:1244–1253. [PubMed: 16728670]
6. Armoundas AA, Hobai IA, Tomaselli GF, Winslow RL, O'Rourke B. Role of sodium-calcium exchanger in modulating the action potential of ventricular myocytes from normal and failing hearts. *Circ Res.* 2003; 93:46–53. [PubMed: 12805237]
7. Shiferaw Y, Sato D, Karma A. Coupled dynamics of voltage and calcium in paced cardiac cells. *Phys Rev E Stat Nonlin Soft Matter Phys.* 2005; 71:021903. [PubMed: 15783348]
8. Restrepo JG, Karma A. Spatiotemporal intracellular calcium dynamics during cardiac alternans. *Chaos.* 2009; 19:037115. [PubMed: 19792040]
9. del Monte F, Lebeche D, Guerrero JL, et al. Abrogation of ventricular arrhythmias in a model of ischemia and reperfusion by targeting myocardial calcium cycling. *Proc Natl Acad Sci U S A.* 2004; 101:5622–5627. [PubMed: 15044708]
10. Ranu HK, Terracciano CM, Davia K, et al. Effects of Na⁽⁺⁾/Ca⁽²⁺⁾-exchanger overexpression on excitation-contraction coupling in adult rabbit ventricular myocytes. *J Mol Cell Cardiol.* 2002; 34:389–400. [PubMed: 11991729]
11. Matsuda T, Arakawa N, Takuma K, et al. Sea0400, a novel and selective inhibitor of the Na⁺-Ca²⁺ exchanger, attenuates reperfusion injury in the in vitro and in vivo cerebral ischemic models. *J Pharmacol Exp Ther.* 2001; 298:249–256. [PubMed: 11408549]
12. Tanaka H, Nishimaru K, Aikawa T, Hirayama W, Tanaka Y, Shigenobu K. Effect of sea0400, a novel inhibitor of sodium-calcium exchanger, on myocardial ionic currents. *Br J Pharmacol.* 2002; 135:1096–1100. [PubMed: 11877314]
13. Kuryshev YA, Wang L, Wible BA, Wan X, Ficker E. Antimony-based antileishmanial compounds prolong the cardiac action potential by an increase in cardiac calcium currents. *Mol Pharmacol.* 2006; 69:1216–1225. [PubMed: 16418337]
14. Luo CH, Rudy Y. A dynamic model of the cardiac ventricular action potential. I. Simulations of ionic currents and concentration changes. *Circ Res.* 1994; 74:1071–1096. [PubMed: 7514509]
15. Mahajan A, Shiferaw Y, Sato D, et al. A rabbit ventricular action potential model replicating cardiac dynamics at rapid heart rates. *Biophys J.* 2008; 94:392–410. [PubMed: 18160660]
16. Kihara Y, Morgan JP. Abnormal Caⁱ²⁺ handling is the primary cause of mechanical alternans: Study in ferret ventricular muscles. *Am J Physiol.* 1991; 261:H1746–H1755. [PubMed: 1750531]
17. Murphy CF, Horner SM, Dick DJ, Coen B, Lab MJ. Electrical alternans and the onset of rate-induced pulsus alternans during acute regional ischaemia in the anaesthetised pig heart. *Cardiovasc Res.* 1996; 32:138–147. [PubMed: 8776411]
18. Orchard CH, McCall E, Kirby MS, Boyett MR. Mechanical alternans during acidosis in ferret heart muscle. *Circ Res.* 1991; 68:69–76. [PubMed: 1984873]
19. Picht E, DeSantiago J, Blatter LA, Bers DM. Cardiac alternans do not rely on diastolic sarcoplasmic reticulum calcium content fluctuations. *Circ Res.* 2006; 99:740–748. [PubMed: 16946134]
20. Walker ML, Wan X, Kirsch GE, Rosenbaum DS. Hysteresis effect implicates calcium cycling as a mechanism of repolarization alternans. *Circulation.* 2003; 108:2704–2709. [PubMed: 14581412]

21. Livshitz LM, Rudy Y. Regulation of Ca^{2+} and electrical alternans in cardiac myocytes: Role of Ca^{2+} and repolarizing currents. *Am J Physiol Heart Circ Physiol.* 2007; 292:H2854–H2866. [PubMed: 17277017]
22. Hund TJ, Otani NF, Rudy Y. Dynamics of action potential head-tail interaction during reentry in cardiac tissue: Ionic mechanisms. *Am J Physiol Heart Circ Physiol.* 2000; 279:H1869–H1879. [PubMed: 11009475]
23. Banyasz T, Fulop L, Magyar J, Szentandrassy N, Varro A, Nanasi PP. Endocardial versus epicardial differences in L-type calcium current in canine ventricular myocytes studied by action potential voltage clamp. *Cardiovasc Res.* 2003; 58:66–75. [PubMed: 12667947]
24. Linz KW, Meyer R. Profile and kinetics of L-type calcium current during the cardiac ventricular action potential compared in guinea-pigs, rats and rabbits. *Pflugers Arch.* 2000; 439:588–599. [PubMed: 10764219]
25. Faber GM, Silva J, Livshitz L, Rudy Y. Kinetic properties of the cardiac L-type Ca^{2+} channel and its role in myocyte electrophysiology: A theoretical investigation. *Biophys J.* 2007; 92:1522–1543. [PubMed: 17158566]
26. Harrison SM, Boyett MR. The role of the Na^{+} - Ca^{2+} exchanger in the rate-dependent increase in contraction in guinea-pig ventricular myocytes. *J Physiol.* 1995; 482(Pt 3):555–566. [PubMed: 7738848]

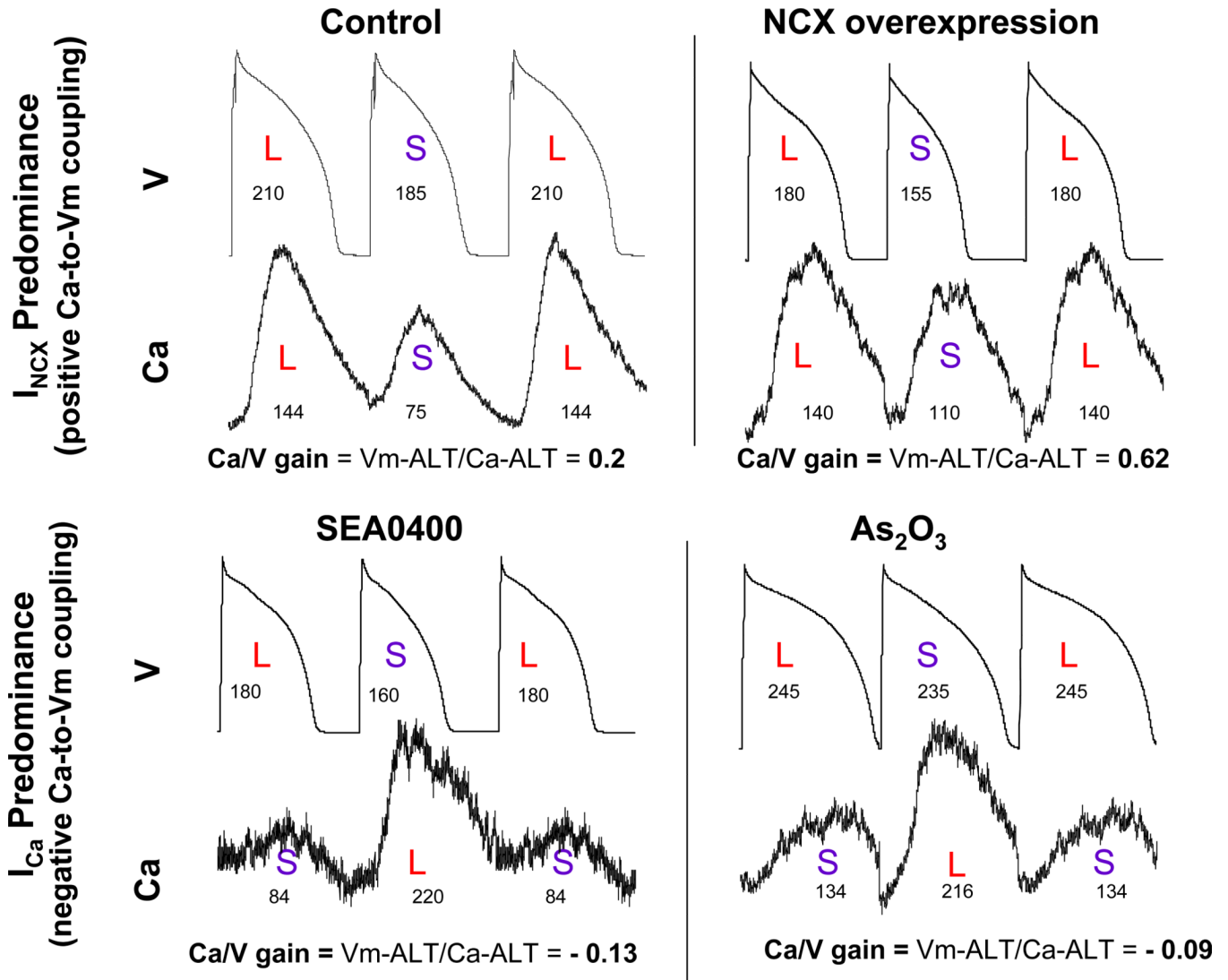


Figure 1. Ca-to-Vm Coupling during alternans is determined by prominence of I_{NCX} versus I_{Ca}
 In control myocyte (top left) Ca-to-Vm coupling was positive; i.e., large Ca transient amplitude was coupled with long APD whereas small Ca transient amplitude was coupled with short APD on subsequent beat. Consistent with this observation, in NCX overexpression myocyte (top right) positive Ca-to-Vm coupling was maintained with concurrent increase in Ca-to-Vm gain, i.e. the ratio of Vm-ALT to Ca-ALT was larger than in control myocyte (0.62 vs 0.2). I_{Ca} predominance created by inhibiting I_{NCX} with SEA0400 (1 μ M) (bottom left) or increasing I_{Ca} with As_2O_3 (bottom right) produced negative Ca-to-Vm coupling at 240 bpm, i.e small Ca transient amplitude was coupled with long APD whereas large Ca transient amplitude was coupled with short APD on subsequent beat. The numbers under action potentials are APD₉₀ (ms) and the numbers under Ca transients are the amplitude of Ca transients (nM).

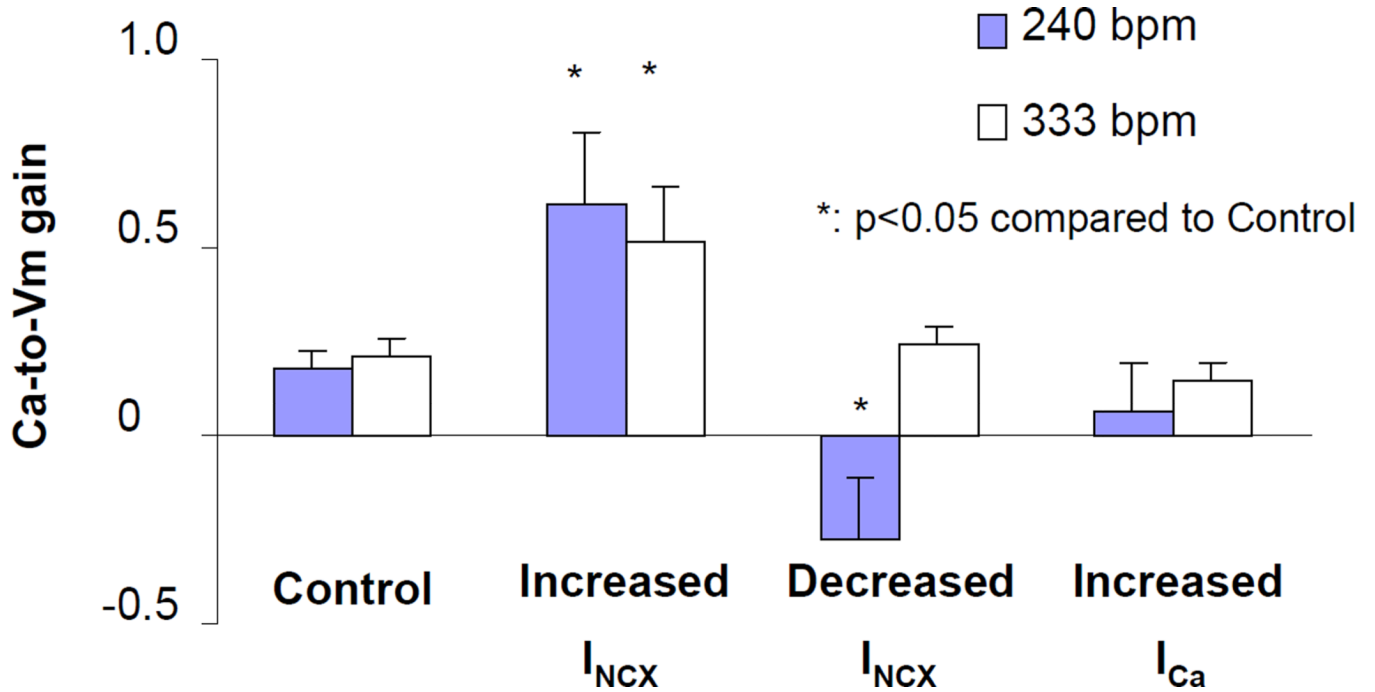


Figure 2. Increasing I_{NCX} predominance increases Ca-to-Vm gain whereas increasing I_{Ca} predominance decreases Ca-to-Vm gain

Ca-to-Vm gain was calculated as the ratio of Vm-ALT to Ca-ALT. The bar graph showed that increasing I_{NCX} predominance by overexpressing NCX increased Ca-to-Vm gain significantly (n=8, p< 0.05 compared to control n=14). At pacing rate of 240 bpm increasing I_{Ca} predominance by inhibiting I_{NCX} with SEA0400 decreased Ca-to-Vm gain significantly (n=11, p< 0.05 compared to control n=14). There was a trend that increasing I_{Ca} with As_2O_3 also decreased Ca-to-Vm gain, but not significantly (n=8, p=0.09 compared to control). However, at faster pacing rate (333 bpm) there was no difference in Ca-to-Vm gain between control and enhancing I_{Ca} predominance groups.

240 bpm (Negative Ca-to-Vm coupling) **333 bpm (Positive Ca-to-Vm coupling)**

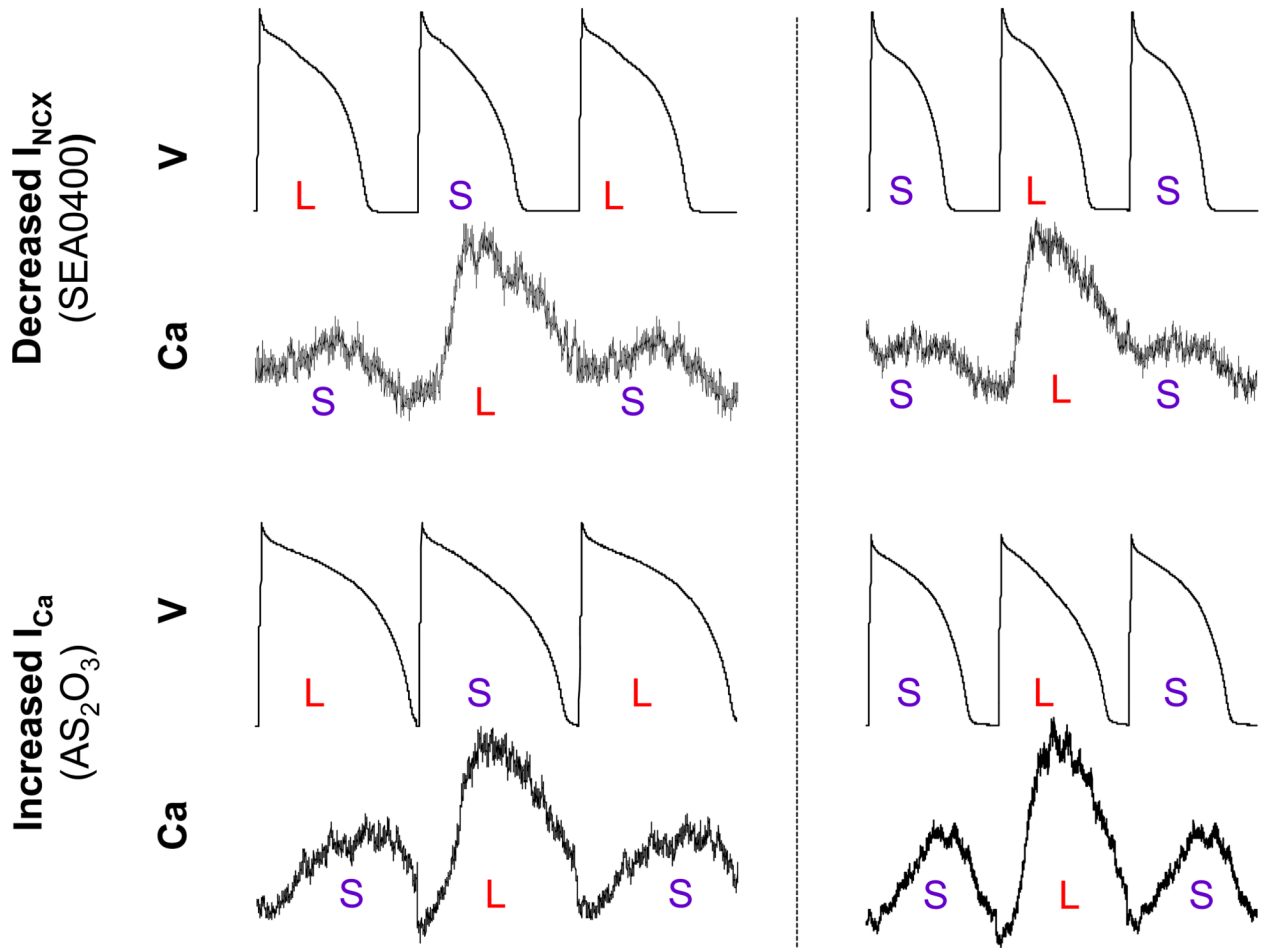


Figure 3. As pacing rate further increased Ca-to-Vm coupling changed from negative coupling to positive coupling in I_{Ca} predominant myocytes
With SEA0400 inhibiting I_{NCX} (top panel) or with As_2O_3 increasing I_{Ca} (bottom panel) Ca-to-Vm coupling was negative at pacing rate of 240 bpm (left). However, as pacing rate increased to 333 bpm Ca-to-Vm coupling changed to positive (right).

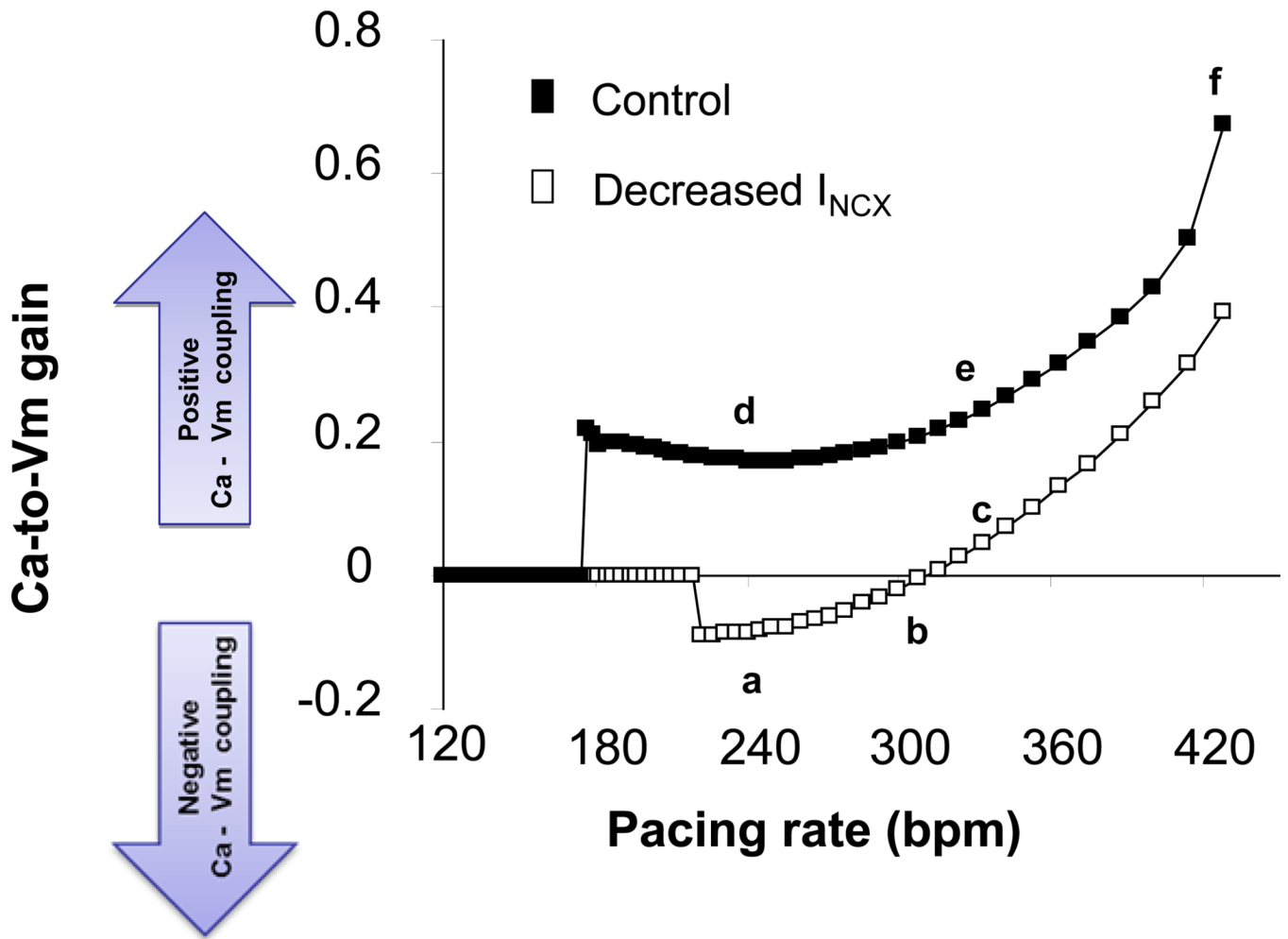


Figure 4. Computer simulations showing that the gain of Ca-to-Vm coupling changed from negative to positive as pacing rate increased

In control alternans occurred when pacing rate reached 180 bpm or faster. Ca-to-Vm coupling was positive. Inhibiting I_{NCX} (by 80%) Ca-to-Vm coupling was negative at pacing rate between 220 and 290 bpm. As pacing rate increased to >300 bpm, Ca-to-Vm coupling changed to positive.

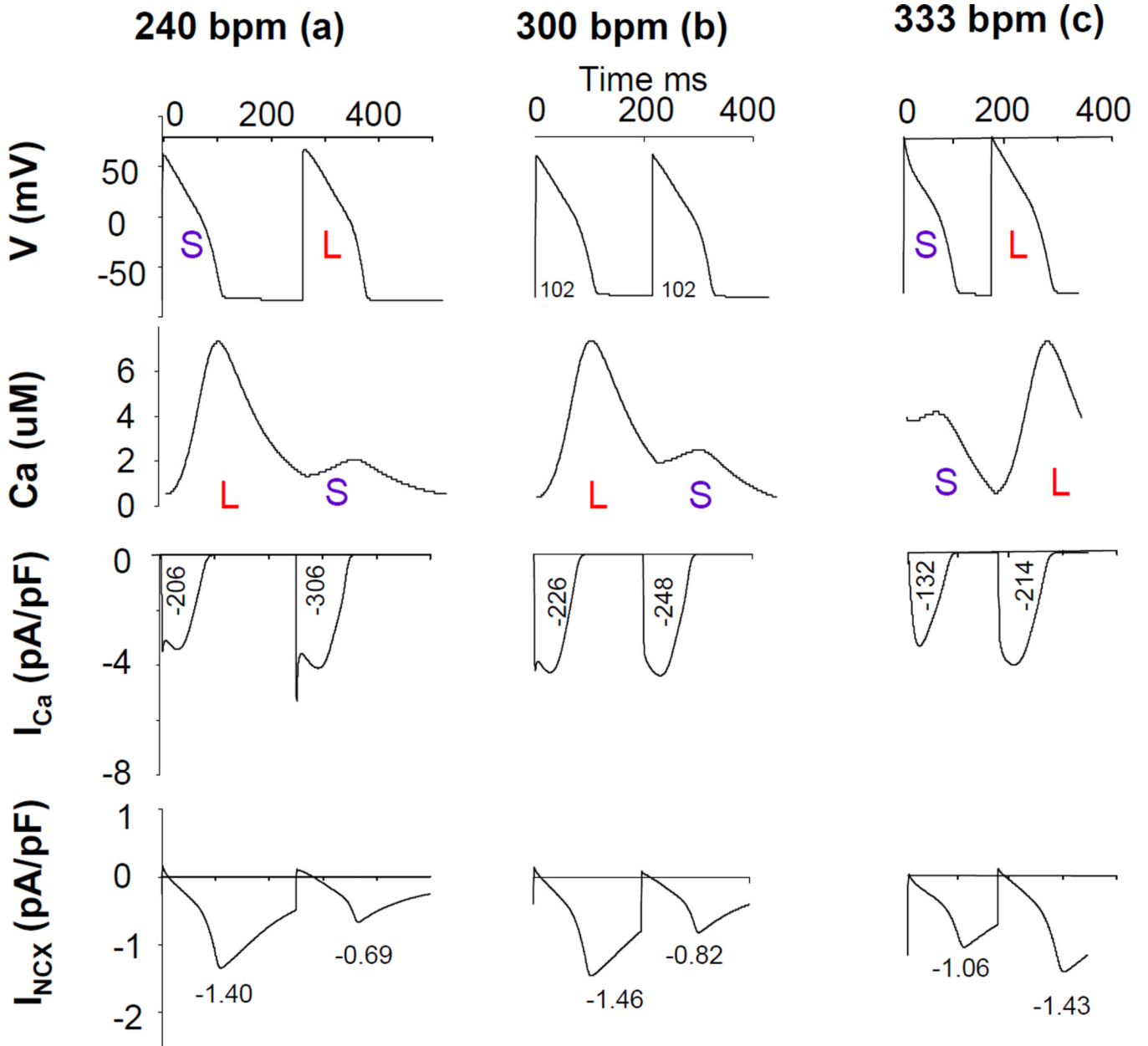


Figure 5. Balanced influence of I_{NCX} and I_{Ca} on Ca-to-Vm coupling in inhibiting I_{NCX} condition

The figure illustrated the traces of action potential, Ca transient, I_{Ca} and I_{NCX} at pacing rate of 240 bpm (left), 300 bpm (middle), and 333 bpm (right) in inhibiting I_{NCX} (by 80%) as shown in Figure 4 (a, b, c) in computer simulation. The numbers under I_{Ca} curves came from the time integration of currents ((pA/pF)*ms), and the numbers under I_{NCX} was the peak current density. Ca-to-Vm coupling was negative with inhibited I_{NCX} at pacing rate of 240 bpm (left). As pacing rate increased to 333 bpm, Ca-to-Vm coupling was positive (right). However, at pacing rate of 300 bpm, there was large Ca-ALT but virtually no Vm-ALT.

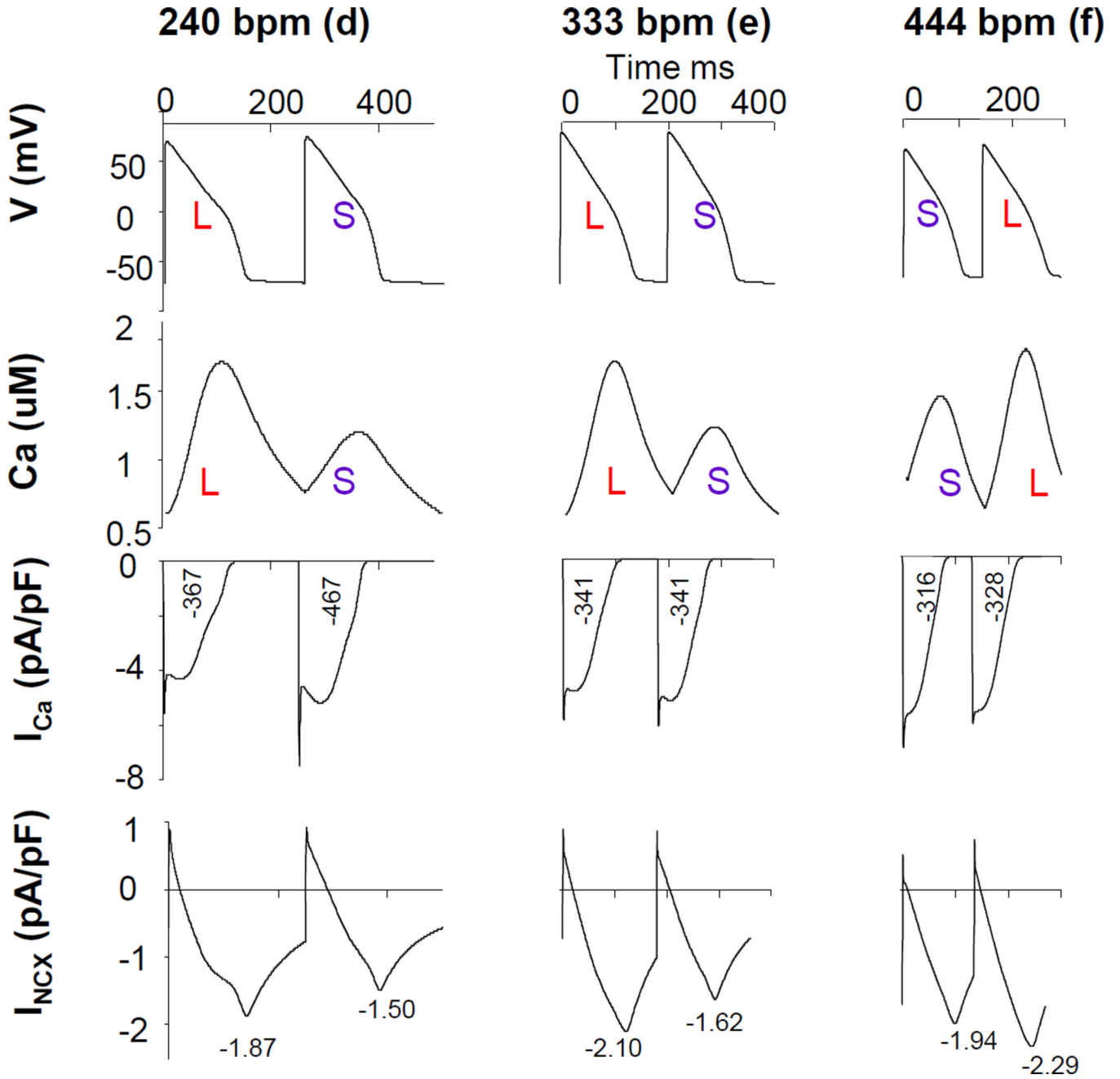


Figure 6. Relationship between Ca-to-Vm coupling and electrogenic currents in control
 The figure illustrated the traces of action potential, Ca transient, I_{Ca} and I_{NCX} at pacing rate of 240 bpm (left), 333 bpm (middle), and 444 bpm (right) in a control as shown in Figure 4 (d, e, f) in computer simulation. Ca-to-Vm coupling were positive at all pacing rate.

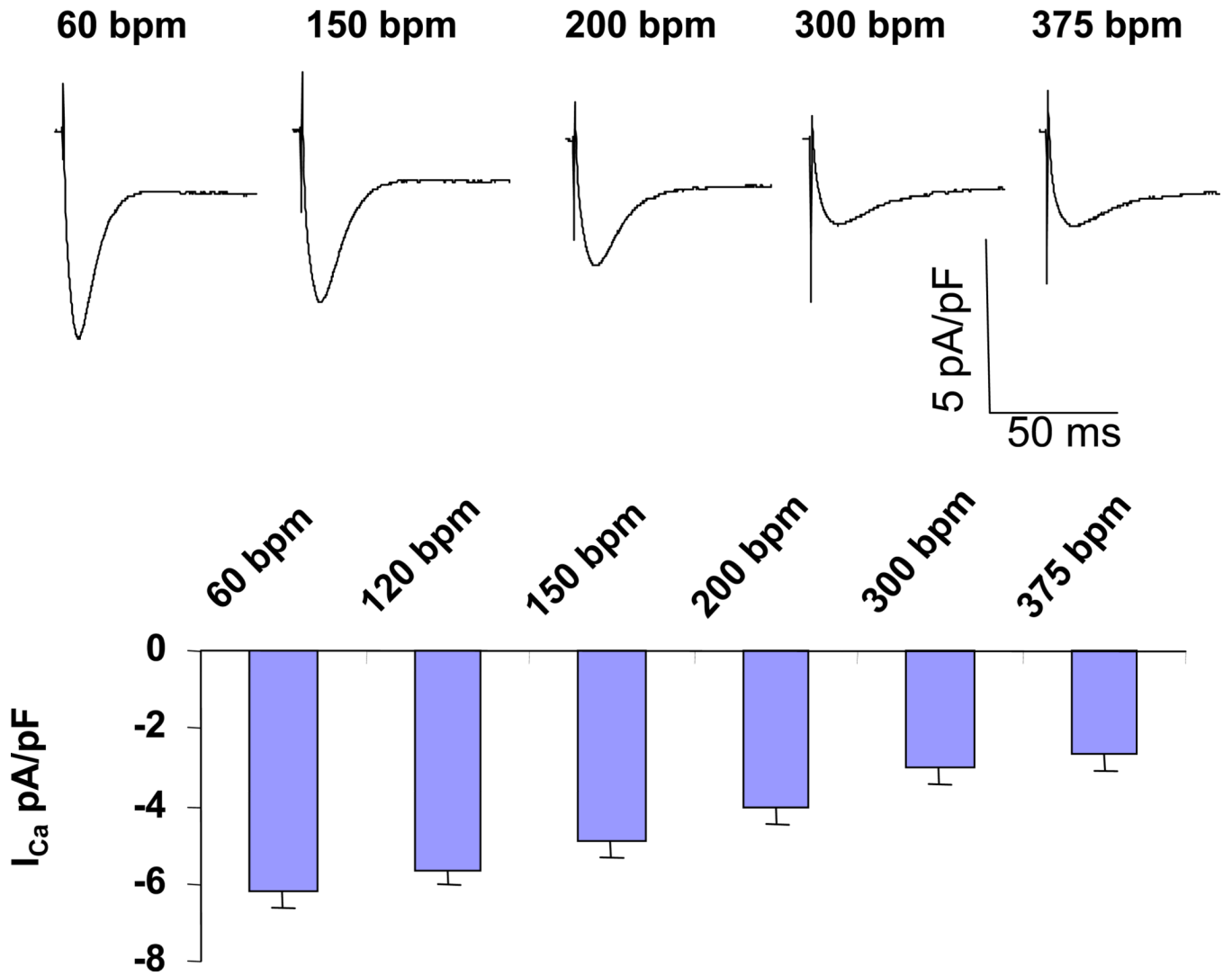


Figure 7. I_{Ca} density decreased as pacing rate increased at fast pacing rate

Top panel illustrated representative traces of I_{Ca} at different pacing rate. As pacing rate increased I_{Ca} density decreased. Summary data from 10 myocytes was shown in bottom panel.

TableEffect of I_{NCX} vs I_{Ca} predominance on Ca-to-Vm coupling.

Predominance	Group	Positive Ca-to-Vm Coupling	Negative Ca-to-Vm Coupling
I_{NCX}	Control	14	0
	Increased I_{NCX}	8	0
	Decreased I_{NCX}	1	10
I_{Ca}	Increased I_{Ca}	4	4